Molecular Therapy
Methods & Clinical Development
Original Article

Nanodysferlins support membrane repair and binding to TRIM72/MG53 but do not localize to t-tubules or stabilize Ca^{2+} signaling

Joaquin Muriel,[1,6] Valeriy Lukyanenko,[1,6] Thomas A. Kwiatkowski,[2,4] Yi Li,[1] Sayak Bhattacharya,[2,5] Kassidy K. Banford,[2] Daniel Garman,[1] Hannah R. Bulgart,[2] Roger B. Sutton,[3] Noah Weisleder,[2] and Robert J. Bloch[1]

[1]Department of Physiology, University of Maryland School of Medicine, Baltimore, MD 21201, USA; [2]Department of Physiology and Cell Biology, The Ohio State University, Columbus, OH 43210, USA; [3]Department of Cell Physiology and Molecular Biophysics, Texas Tech University Health Sciences Center, Lubbock, TX 79430, USA

Mutations in the *DYSF* gene, encoding the protein dysferlin, lead to several forms of muscular dystrophy. In healthy skeletal muscle, dysferlin concentrates in the transverse tubules and is involved in repairing the sarcolemma and stabilizing Ca^{2+} signaling after membrane disruption. The *DYSF* gene encodes 7–8 C2 domains, several Fer and Dysf domains, and a C-terminal transmembrane sequence. Because its coding sequence is too large to package in adeno-associated virus, the full-length sequence is not amenable to current gene delivery methods. Thus, we have examined smaller versions of dysferlin, termed "nanodysferlins," designed to eliminate several C2 domains, specifically C2 domains D, E, and F; B, D, and E; and B, D, E, and F. We also generated a variant by replacing eight amino acids in C2G in the nanodysferlin missing domains D through F. We electroporated dysferlin-null A/J mouse myofibers with Venus fusion constructs of these variants, or as untagged nanodysferlins together with GFP, to mark transfected fibers We found that, although these nanodysferlins failed to concentrate in transverse tubules, three of them supported membrane repair after laser wounding while all four bound the membrane repair protein, TRIM72/MG53, similar to WT dysferlin. By contrast, they failed to suppress Ca^{2+} waves after myofibers were injured by mild hypoosmotic shock. Our results suggest that the internal C2 domains of dysferlin are required for normal t-tubule localization and Ca^{2+} signaling and that membrane repair does not require these C2 domains.

INTRODUCTION

Dysferlin is an integral membrane protein that is missing or mutated in individuals with limb girdle muscular dystrophy type R2 (LGMDR2; formerly LGMD2B and MMD1), as well as other, rarer skeletal myopathies[1–5] (reviewed in[6–12]). The mechanisms underlying the progression of these diseases remains unclear. Several studies support the idea that the absence of functional dysferlin in injured myofibers leads to a defect in sarcolemmal repair,[13–21] which prolongs exposure of the myoplasm to the extracellular milieu and increases cellular damage (reviewed in[22–27]). Other studies suggest that dysferlin is needed to stabilize the biomechanical coupling of the dihydropyridine receptor (DHPR) and the ryanodine receptor (RyR1) that mediates Ca^{2+} release, and that in its absence Ca^{2+} release is compromised, especially when muscle is injured.[28–33] Dysregulation of Ca^{2+} homeostasis in skeletal muscle has been linked to many muscular dystrophies (e.g.,[23–41]). At present, both mechanisms have strong support, and, as they are not mutually exclusive, both may play a role in the pathogenesis. That these two modalities could contribute to myofiber death during dysferlinopathy complicates efforts to develop treatments for these diseases.

Modulating Ca^{2+} signaling with drugs that target the DHPR and RyR1 can suppress Ca^{2+} dysregulation *in vitro* but, with one exception;[28] this approach has not been tested *in vivo*. Exon skipping approaches are not likely to benefit many patients, as the mutations that lead to LGMDR2 are scattered nearly uniformly along the *DYSF* gene (https://databases.lovd.nl/shared/variants). Expressing exogenous dysferlin is difficult, as its open reading frame (ORF) of more than 6,900 bp is too large to package in adeno-associated virus (AAV), which has been used effectively in clinical trials of therapies for other diseases of skeletal muscle (e.g.,[42–45]). To address this, researchers have constructed AAV with portions of the dysferlin cDNA, which when expressed in the same muscle fiber can recombine to generate the complete ORF and restore dysferlin expression.[46–48] Clinical trials of one such approach are now in progress (https://clinicaltrials.gov/ct2/show/NCT02710500?term=dysferlin&cond=LGMD2B&cntry=US&draw=2&rank=1).

Received 10 January 2024; accepted 22 April 2024;
https://doi.org/10.1016/j.omtm.2024.101257.

[4]Present address: Department of Chemistry, West Chester University, West Chester, PA 19383, USA

[5]Present address: NanoString Technologies, Inc., Seattle, WA 98109, USA

[6]These authors contributed equally

Correspondence: Noah Weisleder, Department of Physiology and Cell Biology, The Ohio State University, Columbus, OH 43210, USA.
E-mail: noah.weisleder@OSUMC.edu
Correspondence: Robert J. Bloch, Department of Physiology, University of Maryland School of Medicine, Baltimore, MD 21201, USA.
E-mail: rbloch@umaryland.edu

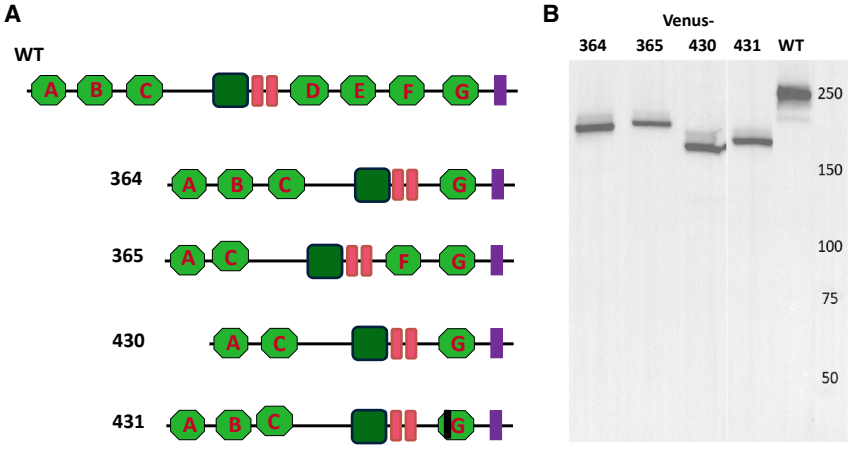

Figure 1. Nanodysferlin structures and mobility in SDS-PAGE

(A) Nanodysferlins: Domains indicated are C2 (light green), C2-FerA (dark green), DysF (red), and transmembrane (purple). The N-terminus, to the left of each structure, was tagged with Venus for some studies. (B) Nanodysferlins tagged with Venus were analyzed by SDS-PAGE and immunoblotted with Hamlet monoclonal antibody against dysferlin.

We have investigated an alternative approach to restoring functional dysferlin to skeletal muscle via AAV transduction: creation of smaller versions of the protein, or "nanodysferlins," that in principle can retain the activities of native dysferlin but that can be packaged in AAV. This approach has been useful in restoring many of the functions of dystrophin in mice and dogs with dystrophinopathies (e.g.,[49–57]). We have shown that some nanodysferlins can support membrane resealing and slow the progression of dysferlinopathy in dysferlin-null mice.[58] Here, we address the ability of additional nanodysferlins to support membrane repair as well as other functions of dysferlin. In particular, we compare the ability of four distinct nanodysferlins to support normal Ca^{2+} signaling in injured dysferlin-null muscle to their ability to facilitate membrane repair and to bind the membrane repair protein, TRIM72/MG53. Our results indicate that three of the four nanodysferlins are effective in membrane repair and that all four bind TRIM72/MG53, but that none stabilize Ca^{2+} signaling.

RESULTS

We prepared four novel nanodysferlins tagged with Venus at their N-termini and expressed them in COS7 or HEK293 cells to ensure that their molecular masses were as predicted and that they were not degraded. Figure 1 presents cartoons of the nanodysferlins (Figure 1A). All contained subsets of dysferlin's C2 domains, while nanodysferlin 431 was a modification of nanodysferlin 430, in which loop 1 of C2G was replaced with the homologous sequence of the helical loop 1 of the cytosolic phospholipase A2 C2 domain.[59] (This loop contains an amphipathic alpha-helix with large hydrophobic residues that can interact with phospholipids). Immunoblots of each are shown in Figure 1B. The results show that the electrophoretic mobilities of nanodysferlins 364, 365, 430, and 431 tagged with Venus (molecular mass, 28 kDa) are in the range expected for their predicted masses of 190, 198, 175, and 190 kDa, respectively.

To test the abilities of the nanodysferlins to target the transverse tubules of skeletal myofibers, we introduced each of these constructs into dysferlin-null A/J mouse muscle fibers by electroporation. Unlike the N-terminal Venus chimera of wild-type (WT) dysferlin, which accumulates in t-tubules,[28,31] nanodysferlins 364 and 430 fail to concentrate in the double lines of puncta at the level of A-I junctions, where the t-tubules are located. Only nanodysferlin 365 and to a lesser extent 431 show occasional puncta at this location (Figure 2, arrowheads, yellow arrowheads; inset shows this is higher magnification). Instead, in the region of the contractile apparatus, the nanodysferlins tend to concentrate at the level of the Z-disks, where Venus alone also concentrates,[31] or in short linear structures centered over Z-disks that extend over adjacent I-bands (Figure 2, white arrowheads), likely to be a compartment of the endoplasmic reticulum (ER).[31] Thus, the nanodysferlins do not accumulate effectively in the site occupied by dysferlin in healthy muscle, the t-tubules.[28,31,60]

To assess membrane repair, we dissected small bundles of fibers and subjected them to laser wounding. (Figure 3). We measured the ability of fibers expressing WT dysferlin or one of the nanodysferlins to take up FM4-64, a dye that associates with the lipid bilayer exposed to the extracellular milieu. Greater dye uptake over time (Figure 3A) in this assay is consistent with slower membrane repair. Our results show that three of the four nanodysferlins only partially restored membrane repair function compared to WT dysferlin (Figures 3B and 3C), with only nanodysferlin 431 being inactive in this assay.

We performed additional experiments with electroporated myofibers that we placed in tissue culture (see Materials and methods). Notably, the nanodysferlins tended to be expressed at lower levels and to be more widely dispersed than WT dysferlin, as indicated by the Venus fluorescence (Fo) (Figure 4, columns of images indicated by *; see also Figure 7). The mean values for their Fo intensities are typically less than one-half of those attained with the WT construct, even when the amount of the WT cDNA used for electroporation is decreased by 2-fold. This suggests that the nanodysferlins do not express well in cultured myofibers.

We assayed the abilities of each of the nanodysferlins to support normal Ca^{2+} signaling in A/J myofibers. We previously showed that WT dysferlin tagged at its N-terminus with Venus could restore normal Ca^{2+} signaling to dysferlin null A/J myofibers in culture, but only in the regions of the fiber where it was expressed. Other regions that were not transfected behaved like untransfected A/J fibers.[30] This was also true when WT dysferlin was expressed at lower levels,

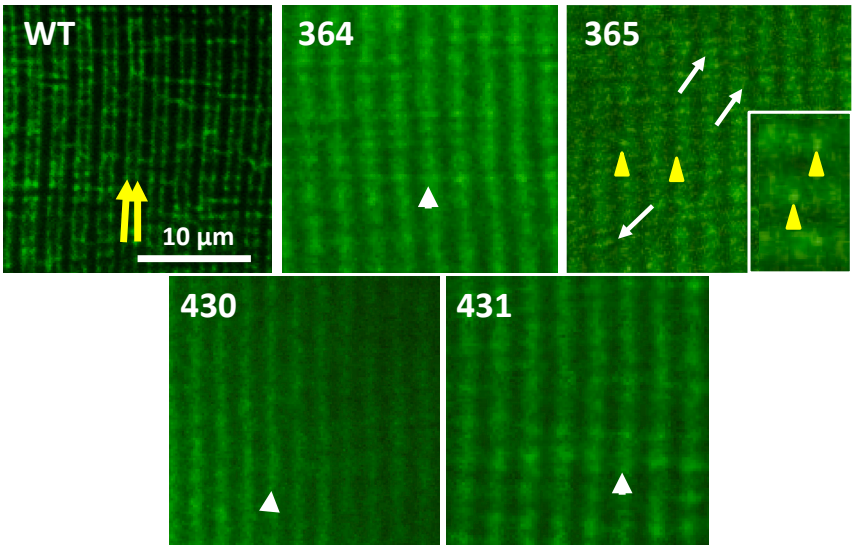

Figure 2. Distribution of nanodysferlins in A/J muscle fibers

FDB muscles of A/J mice were electroporated with Venus constructs of each of the nanodysferlins, and the distribution of the proteins was observed by confocal microscopy. WT dysferlin concentrated in transverse tubules at the level of the A-I junctions (paired yellow arrows). The nanodysferlins concentrated over the Z-disks (364, 430, and 431 arrowheads) or in longitudinal structures that extend over the Z-disks (365, white arrows). Nanodysferlin 365 occasionally accumulates in puncta where transverse tubules might be present (yellow arrowheads). Scale bar, 10 µm.

comparable with the levels of expression of the nanodysferlins studied here (Figure 4; see also Figure 6). Unlike WT-dysferlin, however, none of the nanodysferlins supported normal Ca^{2+} signaling in the regions of the myofibers in which they were expressed. In particular, the amplitude of the Ca^{2+} transient in A/J myofibers before hypo-osmotic shock injury (OSI) was diminished in the presence of nanodysferlin 430 (Figure 5A), and the expression of nanodysferlins 365 and 431 failed to restore the amplitude of the Ca^{2+} transient in A/J myofibers to control levels after OSI (Figure 5B). Recovery of the transient was complete in fibers expressing nanodysferlin 430, but only to the lower level observed before injury. Furthermore, none of the nanodysferlins suppressed Ca^{2+} waves that develop in A/J muscle fibers after injury, with 38%–78% of the transfected fibers showing waves and at frequencies considerably higher than controls (Figures 6C and 6D). Thus, the nanodysferlins do not support normal regulation of Ca^{2+} signaling in A/J myofibers. This was not due to the fact that the nanodysferlins are poorly expressed, as WT dysferlin expressed at similarly low levels was fully active in these assays (Figure 6).

We considered the possibility that the expression of dysferlin with and without an N-terminal Venus moiety might influence the outcome of our assays of membrane repair and Ca^{2+} signaling. Although we observed quantitative differences in our membrane repair assays, the relative differences were maintained (184.6 ± 20.8 area under the curve [AUC] for 364-nanodysferlin + GFP vs. 326.6 ± 40.4 AUC for GFP alone [$p = 0.016$] and 104.8 ± 8.54 AUC for Venus-364-nanodysferlin vs. 286.1 ± 21.3 for GFP alone [$p < 0.0001$]). This difference was not apparent in our Ca^{2+} signaling assays, however (amplitude of the initial transient = 3.8 ± 1.0 arbitrary units for 364-nanodysferlin plus Venus, compared with 4.7 ± 1.7 units for Venus-364-nanodysferlin [$p = 0.095$]; 58% ± 0.2% of recovery of the transient after OSI with 364-nanodysferlin plus Venus, compared with 53% ± 0.2%, with Venus-364-nanodysferlin [$p = 0.47$]; 38% transfected fibers with Ca^{2+} waves for both). Thus, whether it is coupled to Venus or not, nanodysferlin-364 is only partially active in membrane repair and inactive in stabilizing Ca^{2+} signaling.

Finally, we assayed the abilities of the nanodysferlins to interact with the membrane repair protein, TRIM72/MG53. WT dysferlin is known to interact with TRIM72/MG53 to facilitate membrane repair.[16,17,61] We cotransfected HEK293 cells with plasmids encoding EGFP-TRIM72/MG53 and each of the nanodysferlins as Venus chimeras, then prepared cell extracts and performed co-immunoprecipitations with antibodies to TRIM72/MG53, followed by immunoblotting with antibodies to dysferlin and to the EGFP moiety linked to TRIM72/MG53 (NB: We used different solubilization and electrophoresis conditions than for Figure 1B, which account for the reduced mobility of the nanodysferlins constructs shown here). Our results indicated that all the nanodysferlins bound to TRIM72/MG53 specifically, as did WT dysferlin (Figure 7).

DISCUSSION

Dysferlin is a large, multi-domain protein that is required for the health of skeletal muscle, but its functions in healthy muscle and the defects that arise due to its absence are poorly understood. Although its roles in muscle may be diverse, dysferlin is thought to be necessary for at least two, seemingly distinct, cellular processes: the assembly of proteins at the sarcolemma required for the membrane to reseal after injury (membrane repair), and stabilization of interactions among the proteins at the triad junction that regulate the release of Ca^{2+} from the SR stores (Ca^{2+} signaling). Ideally, gene therapies to replace dysferlin when it is missing in human muscle would reconstitute both processes. As most strategies for gene therapy of muscular dystrophies utilize AAV, which has a small packaging size of only approximately 4.4 kb, this approach cannot be used with dysferlin, which has an ORF of >6900 bp. To address this limitation, we designed smaller versions of dysferlin that are lacking different combinations of its structural domains, with the goal of identifying one or more nanodysferlins that would be fully functional. In a previous report, one author showed that several nanodysferlins promoted membrane repair and decreased histopathology in dysferlin-null mice.[58] Here we report that three of four additional

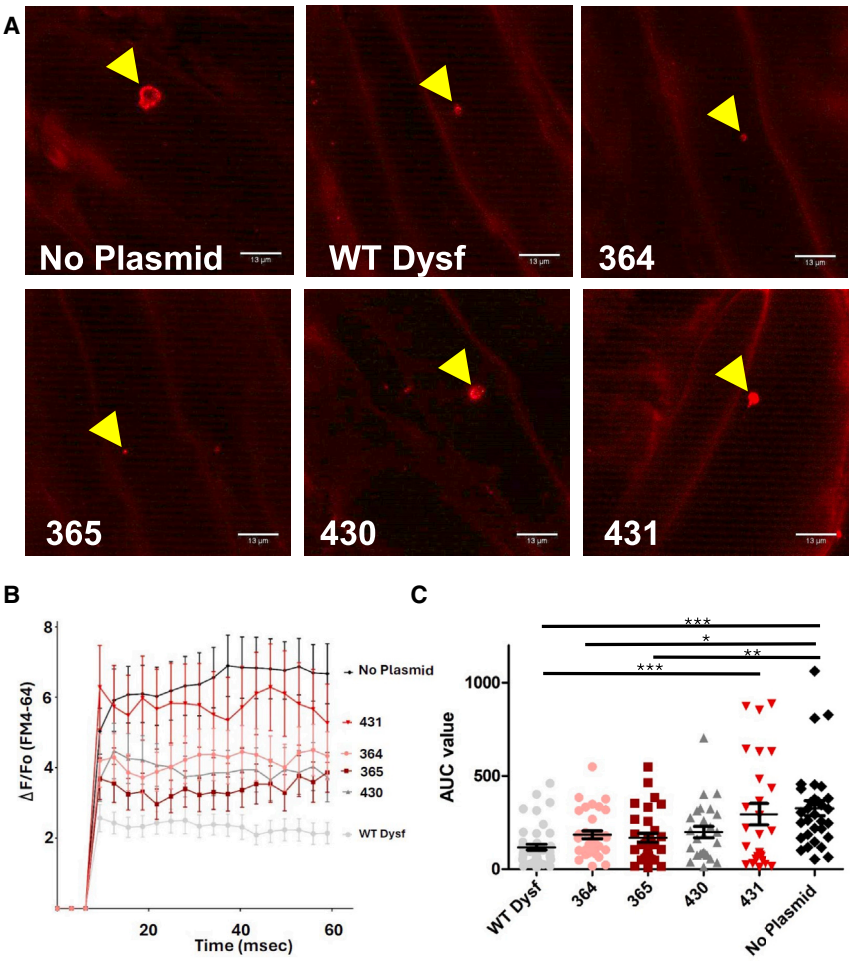

Figure 3. Nanodysferlins 364, 36,5 and 430 restore membrane repair

FDB muscles in dysferlin-deficient A/J mice were electroporated with plasmid DNA constructs expressing various nanodysferlin constructs. After two weeks, muscles were removed and individual muscle fibers were injured by multiphoton infrared confocal microscopy. (A) Fo images of muscle fibers with injury sites (arrows) where external FM4-64 dye enters into the muscle fiber. Lower dye entry indicates improved membrane repair. (B) Time course of FM4-64 dye entry into muscle fibers following injury. Data are presented as means ± SEM. (C) AUC measurements for the values from FM4-64 due entry time course. Each point represented total dye entry for a single injury site in a muscle fiber. Data are presented as means ± SEM. Significance is tested using ANOVA followed by Tukey's post hoc analysis with $^{*}p < 0.05$, $^{**}p < 0.01$, $^{***}p < 0.005$.

nanodysferlins that we have generated can promote membrane repair but that none of them stabilize normal Ca^{2+} signaling.

The principles we followed in designing our nanodysferlins were based on the observation that the most N-terminal and the most C-terminal of dysferlin's C2 domains are essential for activity.[25] Further, we posited that the C2-FerA[62,63] and DysF domains, which are unique to the ferlin family, would be unmodified in the nano constructs. The other five C2 domains and the linker regions between them could be considered for deletion. The nanodysferlins we tested here were similar to those we tested earlier,[58] but differed in their inclusion of all the ferlin and DysF domains and in different combinations of C2 domains. We anticipated that these variants, which are all small enough to express via AAV transduction, would support normal membrane repair and stabilize normal Ca^{2+} signaling.

Our expectations regarding membrane repair were fully borne out. Three of the four nanodysferlins we tested restored membrane repair kinetics to dysferlin-null myofibers injured by laser wounding to values close to those seen with WT dysferlin. The structural features shared by these nanodysferlins are the Fer and Dysf domains, as well as the C2A, C2C, and C2G domains. Thus, the C2B, C2D, C2E, and C2F domains may contribute to optimal membrane repair, but are not required for it to occur, consistent with our earlier results examining the function of specific C2 domains in dysferlin.[31] Replacement of a short amino acid sequence in the C2G domain inhibits nanodysferlin 431 from mediating normal membrane repair. The aim of this design was to replace loop 1 of C2G with a homologous sequence obtained from the helical loop 1 of the cytosolic phospholipase A2 C2 domain.[59] The purpose of this alteration was to address the absence of membrane-interacting C2 domains by enhancing the protein's binding to the membrane through an increase in the hydrophobic residue surface area in C2G. However, the phospholipase A2 loop 1 substitution inhibits nanodysferlin 431 from mediating repair, consistent with an important role for this domain in the process.

Our results measuring the biochemical activity were largely congruent with our results on membrane repair itself. In particular, like WT dysferlin, all the nanodysferlins bound the repair protein, TRIM72/MG53. Each of the nanodysferlins described here contain the C2A domain, which harbors a binding site for TRIM72/MG53.[64] Remarkably, although nanodysferlin 431 also contains the C2A domain and binds TRIM72/MG53, it is inactive in membrane repair, suggesting that binding between dysferlin and TRIM72/MG53 is not sufficient for repair activity. It is also possible that the replacement of eight amino acids in the nanodysferlin 431 construct also alters some functions of the WT protein, perhaps through the creation of unexpected intramolecular interactions within the modified protein.

In contrast with our results with TRIM72/MG53 protein binding and membrane repair, we found that none of the nanodysferlins we tested

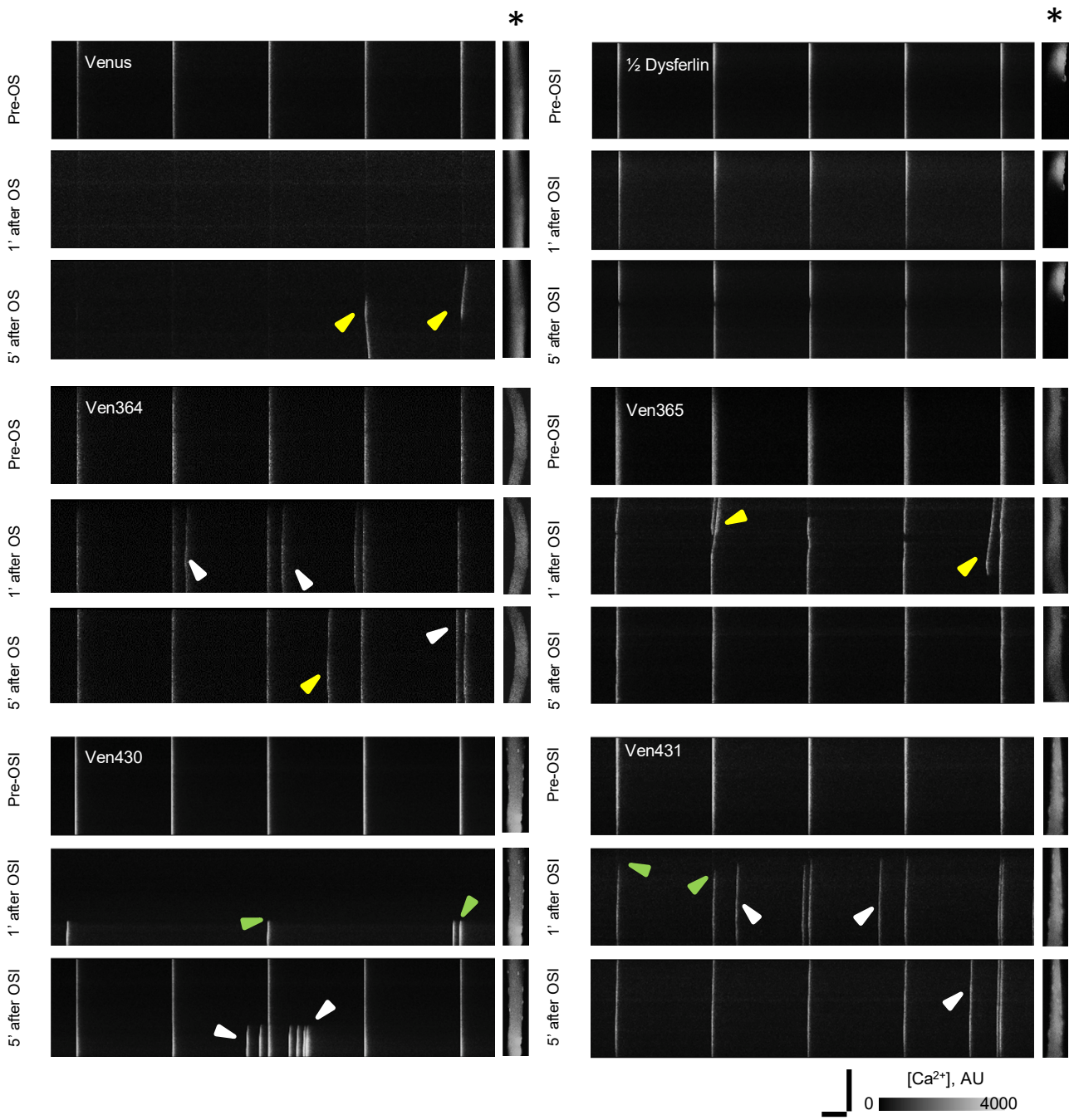

Figure 4. Ca^{2+} transients and Ca^{2+} waves before and after OSI

FDB muscles were transfected and cultured as in Figure 2, but some of the samples were transfected with 0.6 μg instead of 1.2 μg DNA encoding WT dysferlin (1/2 WT Dysf) and others were transfected to express Venus alone. The asterisks (*) indicate columns of images showing the distribution of Venus, dysferlin and the nanodysferlins. After 24 h, fibers were loaded with Rhod2-AM (see Materials and methods) and then electrically stimulated at 1 Hz, to generate the upper panels in each set of three. Fibers were then subjected to a brief OSI and assayed again 1 min and 5 min after being returned to isotonicity, to generate the middle and lower panels in each set. (NB: The small bright spots along the edges of the myofibers expressing nanodysferlins 430 and 431 are likely to be myonuclei, which are surrounded by ER, where these proteins accumulate.) White arrowheads indicate abnormal, spontaneous Ca^{2+} transients; yellow arrowheads indicate transients that are waves, some spontaneous, some evoked; green arrowheads indicate points where the Ca^{2+} transient fails. The results show the appearance of abnormal Ca^{2+} transients, including spontaneous transients and waves, after OSI of myofibers expressing the nanodysferlins.

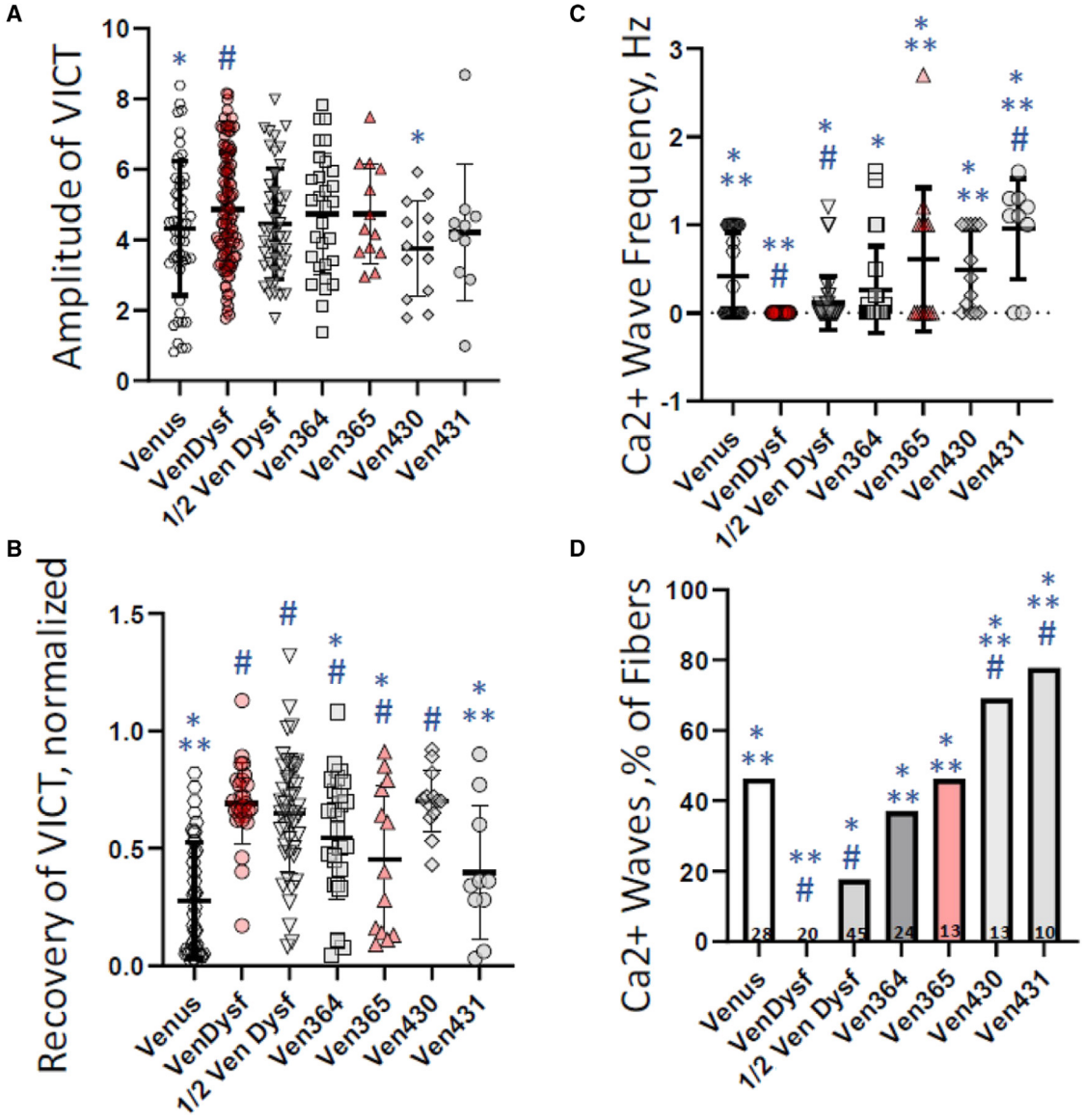

Figure 5. Quantitation of Ca^{2+} transients and waves before and after OSI

Data are shown from a large number of fibers expressing the nanodysferlins, assayed as in Figure 4. (A) Amplitudes of Ca^{2+} transients in transfected myofibers before OSI. (B) Amplitudes of Ca^{2+} transients in transfected myofibers after OSI. (C) Frequencies of Ca^{2+} waves in individual myofibers. (D) Percent of fibers with Ca^{2+} waves. Numbers in the bars indicate the number of fibers examined. Statistically significant differences among experimental constructs and three controls (Dysf, $^1/_2$-Dysf and Venus) were calculated with one-tailed *t* tests and Mann-Whitney *U* statistics, when appropriate (A–C) and A/B statistics (panel D). *$p < 0.05$ compared with Venus-Dysf; **$p < 0.05$ compared with Venus-$^1/_2$ Dysf; #$p < 0.05$ compared with Venus. The results show that Ca^{2+} signaling is abnormal in myofibers expressing nanodysferlin 430 before OSI and all the nanodysferlins after OSI.

supported normal Ca^{2+} signaling by three measures: maintaining the amplitude of the Ca^{2+} transient in uninjured fibers, and promoting the recovery of the Ca^{2+} transient and the suppression of Ca^{2+} waves after osmotic shock injury. (NB: nanodysferlin 430 supported recovery of the transient, but failed to suppress waves.) This defect in stabilization of Ca^{2+} signaling was not due to the fact that the nanodysferlins were expressed at low levels, as low expression of WT dysferlin is sufficient for the complete recovery of the transient and suppression of waves after injury[31] (see also Figure 6). It may, however, be related to the observation that none of the nanodysferlins concentrate at triad junctions nearly as well as WT dysferlin. The concentration of dysferlin in or near the junctional cleft is likely to be important for its ability to stabilize Ca^{2+} signaling.[32]

It is instructional to compare our results with the nanodysferlins with the results of studies of dysferlin variants that lack individual C2

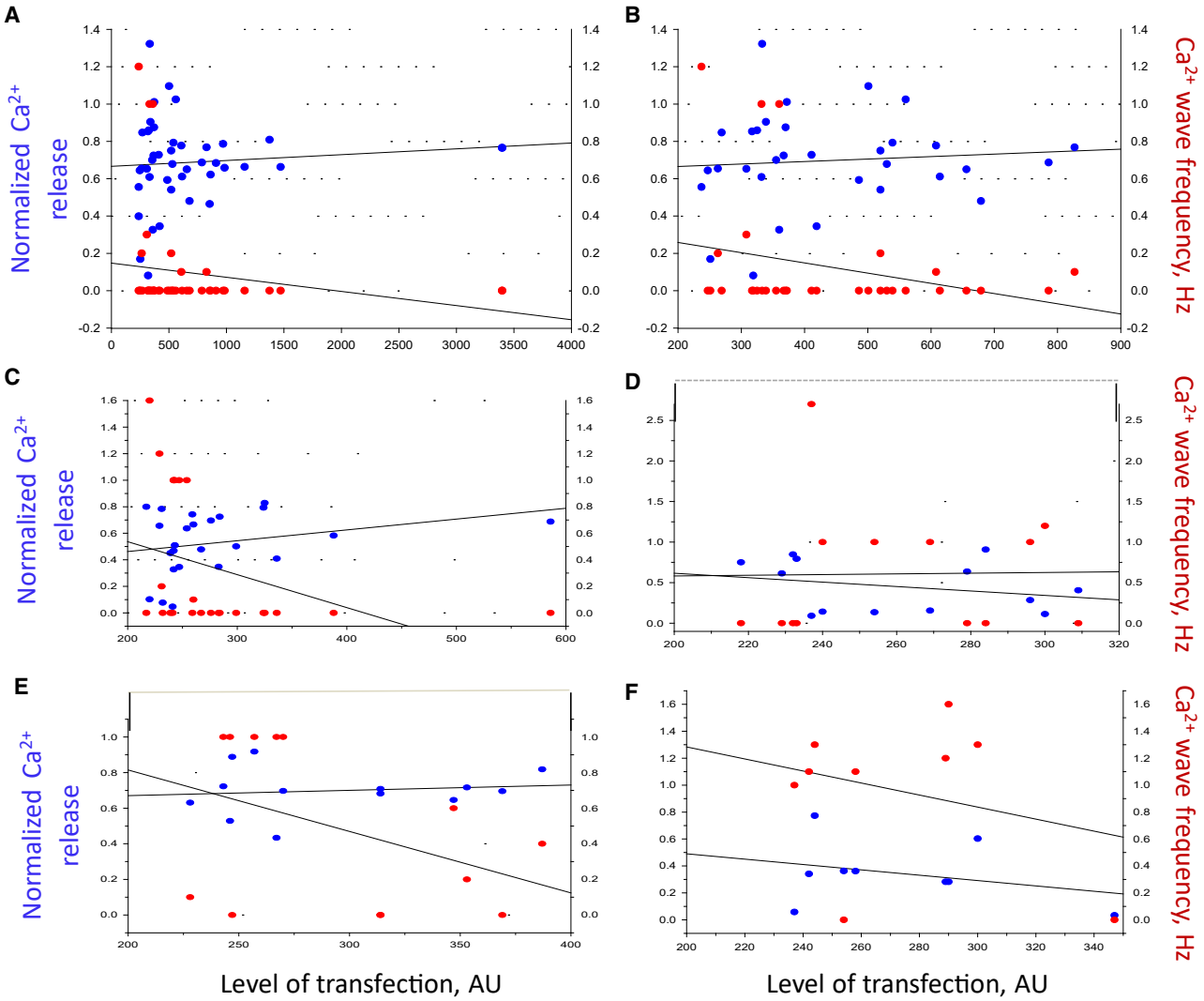

Figure 6. Amplitudes of Ca^{2+} transients and frequency of Ca^{2+} waves as a function of the level of expression of dysferlin and the nanodysferlins

The data in (B) and (D) from Figure 5 were analyzed as a function of the level of Venus Fo in each fiber. (A) WT dysferlin. (B) 1/2 WT dysferlin. (C) Nanodysferlin 364. (D) Nanodysferlin 365. (E) Nanodysferlin 430. (F) Nanodysferlins 431. Note the different scales on the abscissas. The results show that the nanodysferlins are not expressed at nearly the same levels as WT dysferlin or 1/2 WT dysferlin, and that, with the possible exception of nanodysferlin 364, increasing the level of expression of the nanodysferlins does not correct for the defects in Ca^{2+} signaling seen after OSI.

domains.[31] Deletion of either the C2A or C2B domain alone inhibits dysferlin's membrane repair activity, whereas the nanodysferlins lacking the C2B domain (365, 430) partially support membrane repair, as does nanodysferlin 364, which contains the C2B domain. This suggests that the removal of domains C2D and C2E in these constructs allows C2A to function in membrane repair, perhaps along with C2G. Deletion of any of the five more C-terminal C2 domains individually—C2C, C2D, C2E, C2F, or C2G—has an inhibitory effect on membrane repair, especially when either C2F or C2G are missing. (For additional evidence that C2F and C2G play important roles in membrane repair, see.[65]) This suggests that, in truncated variants of dysferlin, C2A and C2B are sufficient to support repair activity if C2F and C2G are also present, although these deletion mutants are less active in repair than WT dysferlin.

By contrast, deletion of C2A or any of dysferlin's five more C-terminal C2 domains individually has profound effects on Ca^{2+} signaling, measured by the recovery of the Ca^{2+} transient after osmotic shock (C2A, C2D–C2G) or the suppression of Ca^{2+} waves (C2C–C2G). The inability of the nanodysferlins to suppress abnormal Ca^{2+} signaling may, therefore, be attributed to the absence of any of these domains. Similarly, the inability of the nanodysferlins to accumulate at triad junctions may be attributed to the absence of two or more of the four C-terminal C2 domains, as deletion of either of these

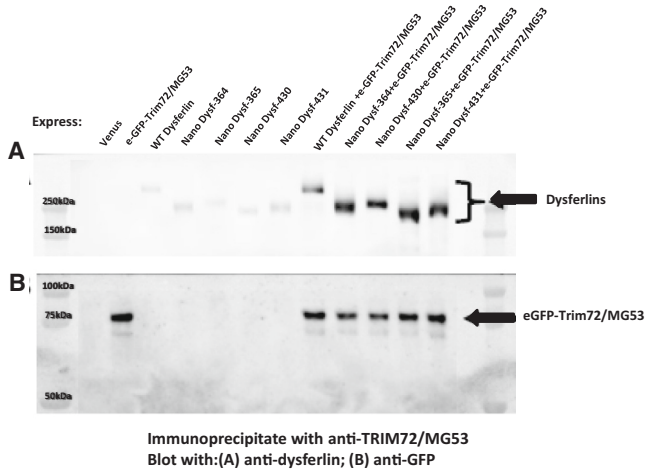

Figure 7. Co-immunoprecipitations of nanodysferlins with TRIM72/MG53

HEK293 cells were co-transfected with expression vectors encoding EGFP-TRIM72/MG53 and Venus fusions of WT dysferlin or one of the nanodysferlins. Whole cell lysates from these cells were immunoprecipitated with anti-TRIM72/MG53 antibody bound to beads. After we subjected the immunoprecipitates to SDS-PAGE and blotting, we probed with anti-dysferlin (A) and anti-GFP (B). The results show that each of the nanodysferlins co-immunoprecipitates with TRIM72/MG53.

domains individually causes the modified dysferlin to accumulate in a compartment of the ER.[31] It is not clear if this is due to changes in the tertiary structure of the protein when C2 domains are missing or if those domains are required for targeting the protein to the transverse tubules and subsequent activity.

It seems clear from these results, as it does from our studies of the deletion of individual C2 domains,[31] that dysferlin variants that exhibit membrane repair activity may fail to support normal Ca^{2+} signaling, and variants that support normal Ca^{2+} signaling may not sustain normal membrane repair. The inability of these nanodysferlins to restore normal Ca^{2+} signaling while still restoring some extent of membrane repair could be one cause of the moderate but not complete prevention of histopathology in dysferlin-deficient mice treated by AAV-mediated overexpression of a nanodysferlins.[58] Restoring one of these processes while not affecting another may not be able to prevent degeneration of the myofiber. However, if the deletion of particular domains can compensate for the absence of others, it may yet be possible to construct a nanodysferlin with full activity in both processes. Finding the appropriate combination of domains will be a very challenging task, however. Alternatively, it may be possible to treat dysferlinopathies with a viral expression vector that encodes a nanodysferlin that supports only one of these functions. A naturally occurring "nanodysferlin," termed by the authors "minidysferlin,"[65] has been identified in an individual that was missing all but the C2F, C2G, and transmembrane domains of dysferlin. At the age of 44, she showed only moderate myopathy.[65] Dysferlin-null mice transduced to express this truncated dysferlin developed muscles that were capable of membrane repair, but that still showed severe histopathology.[65,66] Based on our current results and our earlier work,[31] however, it seems unlikely that omitting one or several C2 domains from dysferlin to enable packaging in AAV will provide a reagent that fully restores membrane repair activity and regulation of Ca^{2+} signaling. Additional research will, therefore, be needed to determine if novel nanodysferlins or versions containing only one or a few of its structural domains can support both Ca^{2+} signaling and membrane repair, and if they correct the pathology in mouse models of dysferlinopathy.

MATERIALS AND METHODS

Mice

Mice were the A/J strain, from Jackson Laboratories (Bar Harbor, ME, USA). Only males were used for these studies, as they respond more reproducibly to injury. *In vivo* transfection of adult skeletal muscle with dysferlin variants with or without a Venus tag, utilized electroporation of flexor digitorum brevis (FDB) muscles, as described for measurements of Ca^{2+} signaling[34,36] and studies of membrane repair.[61,67,68] In experiments in which untagged protein was used, Venus or GFP was co-electroporated to facilitate identification of transfected fibers. All experiments were performed 10–14 days after electroporation to allow for recovery from any damage generated during experimental manipulations. All studies were approved by the Institutional Animal Care and Use Committees of the University of Maryland, Baltimore, and The Ohio State University.

cDNA constructs

Nanodysferlins were prepared as described[58] to generate proteins with the amino acid residues of WT dysferlin, as indicated in Table 1. Deletions were engineered as follows (see Table S1 for primer sequences): Reverse primer anneals with the immediate upstream sequence to the deletion, and forward primer anneals with the sequence immediately downstream to the deletion. The 5′ end of the forward primer is tailed with the sequence immediately upstream to the deletion. Plasmid with full-length dysferlin was used as a template. All variants were expressed as N-terminal Venus fusion proteins, for studies of Ca^{2+} signaling or co-immunoprecipitations with TRIM72/MG53, as well as for some assays of membrane repair.[37]

Constructs for electroporation were tagged with Venus as follows. We introduced restriction sites within the primers (Table S1) and amplified each of the nanodysferlins using the primers carrying the restriction sites. We then digested each of the PCR fragments containing the nanodysferlin ORFs and the Venus-pcDNA plasmid with the restriction enzymes indicated and ligated the products.

Transfection

Transfection of HEK293 and COS7 cells was as described.[37] Expression of the nanodysferlins as Venus fusion proteins was assayed by SDS-PAGE, transfer to PVDF membrane, and immunoblotting with Hamlet anti-dysferlin, as reported.[31] Prior to electrophoresis, cell pellets were extracted with RIPA buffer. The extracts were incubated with three volumes of 2× concentrated SDS-PAGE sample buffer for 15 min at 37°C and analyzed in 4%–12% Bis-Tris

Table 1. Nanodysferlins tested

Nanodysferlin variant	Amino acids included[a]	Amino acids deleted[a]	Other changes[a]
364	1–1,136; 1,789–2,080	1,137–1–788	C1232A; C1290A
365	1–218; 366–1136; 1,579–2,080	219–365; 1,137–1,578	C1232A; C1290A
430	1–218; 357–1,136; 1,789–2,080	219–365; 1,137–1,578	C1232A; C1290A
435	1–1,136; 1,789–2,080	1,137–1,788	C1232A; C1290A; TKGAFGDMLDTP replaces 1,824–1,836

[a]Amino acid residues are numbered according to human dysferlin, isoform 8: (NP_003485).

acrylamide gels in MES running buffer (all reagents from BioRad, Hercules, CA, USA).

FDB muscles were transfected by electroporation, as described.[30,31,68,69] Muscles were removed 1–2 weeks after electroporation and either dissociated and cultured on a layer of Matrigel (Sigma-Aldrich, St. Louis, MO, USA) to study Ca^{2+} signaling and t-tubule localization, or teased into small bundles to assess membrane repair.

Membrane repair

Membrane repair was assayed as reported.[61,67] Briefly, FDB muscles were surgically isolated 2 weeks after electroporation and placed in Ca^{2+}-free Tyrode solution (140 mM NaCl, 5 mM KCl, 2 mM $MgCl_2$, 10 mM HEPES, pH 7.2). Muscle bundles were mechanically separated at the tendon and then adhered on glass-bottomed culture dishes (MatTek, Ashland, MA, USA) with Liquid Bandage (New Skin, Tarrytown, NY, USA) applied to the exposed tendons. Membrane disruption was induced in Tyrode supplemented with 2.5 μM FM4-64 dye (Thermo Fisher Scientific, Waltham, MA, USA), and in either 2 mM Ca^{2+} or 2 mM EGTA, with a FluoView FV1000 multi-photon confocal laser-scanning microscope (Olympus, Center Valley, PA, USA). A 2.5-μm circular region of interest was selected along the edge of the sarcolemma and irradiated with a DeepSee MaiTai titanium-sapphire laser at a wavelength of 800 nm and 10% of maximum infrared laser power for 3 s. Images were captured before and after damage every 5 s for a total of 60 s. Images were analyzed with ImageJ Fiji (National Institutes of Health, Bethesda, MD, USA), by measuring the Fo intensity in a region of interest encompassing the entire area of dye uptake, with results represented as ΔF/Fo. The AUC and the peak FM4-64 intensity were calculated with GraphPad Prism software (GraphPad Software, La Jolla, CA, USA).

Ca^{2+} release

Events were assayed as described.[30] In brief, myofibers from electroporated FDB muscles were isolated, placed into tissue culture and loaded with Rhod-2AM (Thermo Fisher Scientific), as described.[30,31] They were then placed under confocal illumination (Zeiss Duo, Jena, Germany) and subjected to trains of electrical stimulation (1 Hz for 10 s) to evoke Ca^{2+} transients every 1 min. Excitation was at 560 nm and emission was measured at more than 575 nm, set with an LP 575 filter. With the aperture of the confocal detector set at maximum to image the middle of myofibers, line scan images were acquired at a rate of 1.9 ms/line. ImageJ 1.31v (National Institutes of Health) was used to determine the mean maximal value of the Ca^{2+} transients, as the difference between maximal Fo intensity and background Fo, normalized to Fo. For OSI, fibers were superfused for 1 min with a hypotonic Tyrode's solution containing only 70 mM NaCl, then returned to isotonic Tyrode's solution for 5 min. All studies were done at ambient temperature (21°C–23°C).

Levels of transfection

Levels of transfection were assessed as the Venus Fo in myofibers before Rhod-2 imaging, as described.[32] Gains were adjusted to obtain an average cell auto Fo in the Venus channel of 200 arbitrary units (AU; maximum = 4,095 AU). Venus Fo intensity was measured from 100 pixels per cell with ImageJ 1.31v (National Institutes of Health).

Co-immunoprecipitation

COS7 cells (70% confluent, on 10-cm plastic tissue culture dishes) were transfected with 1 part Lipofectamine 2000 to 2 parts cDNA encoding Venus-dysferlin or each of the Venus-nanodysferlins (9 μg/plate), Venus alone (1 μg/plate), EGFP-TRIM72/MG53 alone (1 μg/plate), or a combination of EGFP-TRIM72/MG53 and one of the Venus-dysferlin constructs with EGFP-TRIM72/MG53 in a ratio 9:1, for a total of 10 μg/plate. Cell extracts were prepared 1 day later. Immunoprecipitates were generated from 200 μg cell protein with 15 μL rabbit anti-TRIM72/MG53 antibody produced in the Weisleder laboratory.[70] Beads containing the immunoprecipitates were eluted with 2× concentrated SDS-PAGE sample buffer at room temperature for 10 min, then incubated at 37°C for 15 min before electrophoresis in 4%–12% gels with MES running buffer. (NB: Extracts of cells expressing Venus-dysferlin that were treated identically showed greater mobility upon electrophoresis.) After SDS-PAGE, transfer to nitrocellulose paper and incubation in blocking solution, blots were probed with Hamlet mouse monoclonal anti-dysferlin (Leica Biosystems, Deer Park, IL, USA), diluted 1:1,000, and mouse monoclonal anti-GFP (Sigma-Aldrich, St. Louis, MO, USA), diluted 1:1,000. Blots were developed with SuperSignal West Femto Maximum Sensitivity Substrate (Thermo Fisher Scientific) and imaged on a Biorad ChemiDoc MP.

Statistics

Statistics were analyzed with Prism or SigmaPlot 13.0 software, with a p value of less than 0.05 considered significant. Statistical analysis of

the data obtained from assays of laser injury was performed by one-way ANOVA, comparing the mean AUC of time over the change in the Fo curves for individual muscle fibers from each group. All data were collected from muscles or myofibers from three or more mice and are displayed as mean ± SE.

Materials

Materials were from Sigma-Aldrich and Thermo Fisher Scientific unless otherwise noted.

DATA AND CODE AVAILABILITY

The data generated in this study are available upon request.

SUPPLEMENTAL INFORMATION

Supplemental information can be found online at https://doi.org/10.1016/j.omtm.2024.101257.

ACKNOWLEDGMENTS

This research was supported by grants from the National Institutes of Health (R56 AR078800 to N.W.; 2 RO1 AR064268 to R.J.B.), from the Jain Foundation to R.B.S., N.W., and R.J.B., and by a stipend from T32 AR007592 (principal investigator, A. Kontrogianni-Konstantopoulos) to D.G.

AUTHOR CONTRIBUTIONS

J.M. created the Venus-nanodysferlin constructs, electroporated them into muscle cultured muscle fibers and analyzed their distribution in the cultured fibers. V.L. analyzed the effects of the nanodysferlins on Ca^{2+} signaling. L.Y. and H.B. studied the association of TRIM72/MG53 with the nanodysferlins. D.G. determined the molecular sizes of the nanodysferlins. T.K., S.B., and K.B. studied the effects of the nanodysferlins on sarcolemmal membrane repair. R.B.S. designed the nanodysferlins and edited the paper. N.W. supervised the studies of sarcolemmal membrane repair and binding of the nanodysferlins to TRIM72/MG53, and edited the paper. R.J.B. helped to supervise the studies of TRIM72/MG53 binding to the nanodysferlins, supervised the studies of the subcellular targeting of the nanodysferlins and their ability to restore normal Ca^{2+} signaling in dysferlin-null myofibers, and wrote the paper.

DECLARATION OF INTERESTS

The authors declare no competing interests.

REFERENCES

1. Passos-Bueno, M.R., Moreira, E.S., Marie, S.K., Bashir, R., Vasquez, L., Love, D.R., Vainzof, M., Iughetti, P., Oliveira, J.R., Bakker, E., et al. (1996). Main clinical features of the three mapped autosomal recessive limb-girdle muscular dystrophies and estimated proportion of each form in 13 Brazilian families. Med. Genet. *33*, 97–102.
2. Bashir, R., Britton, S., Strachan, T., Keers, S., Vafiadaki, E., Lako, M., Richard, I., Marchand, S., Bourg, N., Argov, Z., et al. (1998). A gene related to *Caenorhabditis elegans* spermatogenesis factor *fer-1* is mutated in limb-girdle muscular dystrophy type 2B. Nat. Genet. *20*, 37–42.
3. Liu, J., Aoki, M., Illa, I., Wu, C., Fardeau, M., Angelini, C., Serrano, C., Urtizberea, J.A., Hentati, F., Hamida, M.B., et al. (1998). Dysferlin, a novel skeletal muscle gene, is mutated in Miyoshi myopathy and limb girdle muscular dystrophy. Nat. Genet. *20*, 31–36.
4. Aoki, M., Arahata, K., and Brown, R.H., Jr. (1999). Positional cloning of the gene for Miyoshi myopathy and limb-girdle muscular dystrophy. Rinsho Shinkeigaku *39*, 1272–1275.
5. Illarioshkin, S.N., Ivanova-Smolenskaya, I.A., Greenberg, C.R., Nylen, E., Sukhorukov, V.S., Poleshchuk, V.V., Markova, E.D., and Wrogemann, K. (2000). Identical dysferlin mutation in limb-girdle muscular dystrophy type 2B and distal myopathy. Neurology *55*, 1931–1933.
6. Bushby, K.M. (2000). Dysferlin and muscular dystrophy. Acta Neurol. Belg. *100*, 142–145.
7. Aoki, M., and Takahashi, T. (2004). Dysferlinopathy. In GeneReviews(®), M.P. Adam, J. Feldman, G.M. Mirzaa, R.A. Pagon, S.E. Wallace, L.J.H. Bean, K.W. Gripp, and A. Amemiya, eds. (University of Washington).
8. Urtizberea, J.A., Bassez, G., Leturcq, F., Nguyen, K., Krahn, M., and Levy, N. (2008). Dysferlinopathies. Neurol. India *56*, 289–297.
9. Amato, A.A., and Brown, R.H., Jr. (2011). Dysferlinopathies. Handb. Clin. Neurol. *101*, 111–118.
10. Fanin, M., and Angelini, C. (2016). Progress and challenges in diagnosis of dysferlinopathy. Muscle Nerve *54*, 821–835.
11. Moore, U., Gordish, H., Diaz-Manera, J., James, M.K., Mayhew, A.G., Guglieri, M., Fernandez- Torron, R., Rufibach, L.E., Feng, J., Blamire, A.M., et al. (2021). Miyoshi myopathy and limb girdle muscular dystrophy R2 are the same disease. Neuromuscul. Disord. *31*, 265–280.
12. Ivanova, A., Smirnikhina, S., and Lavrov, A. (2022). Dysferlinopathies: Clinical and genetic variability. Clin. Genet. *102*, 465–473.
13. Lennon, N.J., Kho, A., Bacskai, B.J., Perlmutter, S.L., Hyman, B.T., and Brown, R.H., Jr. (2003). Dysferlin interacts with annexins A1 and A2 and mediates sarcolemmal wound-healing. J. Biol. Chem. *278*, 50466–50473.
14. Bansal, D., Miyake, K., Vogel, S.S., Groh, S., Chen, C.C., Williamson, R., McNeil, P.L., and Campbell, K.P. (2003). Defective membrane repair in dysferlin-deficient muscular dystrophy. Nature *423*, 168–172.
15. Ho, M., Post, C.M., Donahue, L.R., Lidov, H.G.W., Bronson, R.T., Goolsby, H., Watkins, S.C., Cox, G.A., and Brown, R.H., Jr. (2004). Disruption of muscle membrane and phenotype divergence in two novel mouse models of dysferlin deficiency. Hum. Mol. Genet. *13*, 1999–2010.
16. Cai, C., Weisleder, N., Ko, J.K., Komazaki, S., Sunada, Y., Nishi, M., Takeshima, H., and Ma, J. (2009). Membrane repair defects in muscular dystrophy are linked to altered interaction between MG53, caveolin-3, and dysferlin. J. Biol. Chem. *284*, 15894–15902.
17. Lek, A., Evesson, F.J., Lemckert, F.A., Redpath, G.M.I., Lueders, A.K., Turnbull, L., Whitchurch, C.B., North, K.N., and Cooper, S.T. (2013). Calpains, cleaved mini-dysferlinC72, and L-type channels underpin calcium-dependent muscle membrane repair. J. Neurosci. *33*, 5085–5094.
18. McDade, J.R., and Michele, D.E. (2014). Membrane damage-induced vesicle-vesicle fusion of dysferlin-containing vesicles in muscle cells requires microtubules and kinesin. Hum. Mol. Genet. *23*, 1677–1686.
19. McDade, J.R., Archambeau, A., and Michele, D.E. (2014). Rapid actin-cytoskeleton-dependent recruitment of plasma membrane-derived dysferlin at wounds is critical for muscle membrane repair. Faseb. J. *28*, 3660–3670.
20. Demonbreun, A.R., Quattrocelli, M., Barefield, D.Y., Allen, M.V., Swanson, K.E., and McNally, E.M. (2016). An actin-dependent annexin complex mediates plasma membrane repair in muscle. J. Cell Biol. *213*, 705–718.
21. Bittel, D.C., Chandra, G., Tirunagri, L.M.S., Deora, A.B., Medikayala, S., Scheffer, L., Defour, A., and Jaiswal, J.K. (2020). Annexin A2 mediates dysferlin accumulation and muscle cell membrane repair. Cells *9*, 1919.
22. Doherty, K.R., and McNally, E.M. (2003). Repairing the tears: dysferlin in muscle membrane repair. Trends Mol. Med. *9*, 327–330.
23. Bansal, D., and Campbell, K.P. (2004). Dysferlin and the plasma membrane repair in muscular dystrophy. Trends Cell Biol. *14*, 206–213.
24. Glover, L., and Brown, R.H., Jr. (2007). Dysferlin in membrane trafficking and patch repair. Traffic *8*, 785–794.

25. Cooper, S.T., and Head, S.I. (2015). Membrane injury and repair in the muscular dystrophies. Neuroscientist *21*, 653–668.

26. Demonbreun, A.R., and McNally, E.M. (2016). Plasma membrane repair in health and disease. Curr. Top. Membr. *77*, 67–96.

27. Barthélémy, F., Defour, A., Lévy, N., Krahn, M., and Bartoli, M. (2018). Muscle Cells Fix Breaches by Orchestrating a Membrane Repair Ballet. J. Neuromuscul. Dis. *5*, 21–28.

28. Kerr, J.P., Ziman, A.P., Mueller, A.L., Muriel, J.M., Kleinhans-Welte, E., Gumerson, J.D., Vogel, S.S., Ward, C.W., Roche, J.A., and Bloch, R.J. (2013). Dysferlin stabilizes stress-induced Ca^{2+} signaling in the transverse tubule membrane. Proc. Natl. Acad. Sci. USA *110*, 20831–20836.

29. Kerr, J.P., Ward, C.W., and Bloch, R.J. (2014). Dysferlin at transverse tubules regulates Ca(2+) homeostasis in skeletal muscle. Front. Physiol. *5*, 89.

30. Lukyanenko, V., Muriel, J.M., and Bloch, R.J. (2017). Coupling of excitation to Ca(2+) release is modulated by dysferlin. J. Physiol. *595*, 5191–5207.

31. Muriel, J., Lukyanenko, V., Kwiatkowski, T., Bhattacharya, S., Garman, D., Weisleder, N., and Bloch, R.J. (2022). The C2 domains of dysferlin: roles in membrane localization, Ca(2+) signalling and sarcolemmal repair. J. Physiol. *600*, 1953–1968.

32. Lukyanenko, V., Muriel, J., Garman, D., Breydo, L., and Bloch, R.J. (2022). Elevated Ca(2+) at the triad junction underlies dysregulation of Ca(2+) signaling in dysferlin-null skeletal muscle. Front. Physiol. *13*, 1032447.

33. Kar, N.C., and Pearson, C.M. (1978). Muscular dystrophy and activation of proteinases. Muscle Nerve *1*, 308–313.

34. Gommans, I.M.P., Vlak, M.H.M., de Haan, A., and van Engelen, B.G.M. (2002). Calcium regulation and muscle disease. J. Muscle Res. Cell Motil. *23*, 59–63.

35. Bellinger, A.M., Reiken, S., Dura, M., Murphy, P.W., Deng, S.X., Landry, D.W., Nieman, D., Lehnart, S.E., Samaru, M., LaCampagne, A., and Marks, A.R. (2008). Remodeling of ryanodine receptor complex causes "leaky" channels: a molecular mechanism for decreased exercise capacity. Proc. Natl. Acad. Sci. USA *105*, 2198–2202.

36. Burr, A.R., and Molkentin, J.D. (2015). Genetic evidence in the mouse solidifies the calcium hypothesis of myofiber death in muscular dystrophy. Cell Death Differ. *22*, 1402–1412.

37. Avila, G. (2018). Disturbed Ca(2+) Homeostasis in Muscle-Wasting Disorders. Adv. Exp. Med. Biol. *1088*, 307–326.

38. Lawal, T.A., Todd, J.J., Witherspoon, J.W., Bönnemann, C.G., Dowling, J.J., Hamilton, S.L., Meilleur, K.G., and Dirksen, R.T. (2020). Ryanodine receptor 1-related disorders: an historical perspective and proposal for a unified nomenclature. Skeletal Muscle *10*, 32.

39. Mareedu, S., Million, E.D., Duan, D., and Babu, G.J. (2021). Abnormal calcium handling in Duchenne muscular dystrophy: Mechanisms and potential therapies. Front. Physiol. *12*, 647010.

40. Zabłocka, B., Górecki, D.C., and Zabłocki, K. (2021). Disrupted calcium homeostasis in Duchenne muscular dystrophy: A common mechanism behind diverse consequences. Int. J. Mol. Sci. *22*, 11040.

41. Michelucci, A., Liang, C., Protasi, F., and Dirksen, R.T. (2021). Altered Ca(2+) handling and oxidative stress underlie mitochondrial damage and skeletal muscle dysfunction in aging and disease. Metabolites *11*, 424.

42. Smith, B.K., Collins, S.W., Conlon, T.J., Mah, C.S., Lawson, L.A., Martin, A.D., Fuller, D.D., Cleaver, B.D., Clément, N., Phillips, D., et al. (2013). Phase I/II trial of adeno-associated virus- mediated alpha-glucosidase gene therapy to the diaphragm for chronic respiratory failure in Pompe disease: initial safety and ventilatory outcomes. Hum. Gene Ther. *24*, 630–640.

43. Smith, B.K., Martin, A.D., Lawson, L.A., Vernot, V., Marcus, J., Islam, S., Shafi, N., Corti, M., Collins, S.W., and Byrne, B.J. (2017). Inspiratory muscle conditioning exercise and diaphragm gene therapy in Pompe disease: Clinical evidence of respiratory plasticity. Exp. Neurol. *287*, 216–224.

44. Duan, D. (2018). Systemic AAV Micro-dystrophin gene tyherapy for Duchenne Muscular Dystrophy. Mol. Ther. *26*, 2337–2356.

45. Mendell, J.R., Sahenk, Z., Lehman, K., Nease, C., Lowes, L.P., Miller, N.F., Iammarino, M.A., Alfano, L.N., Nicholl, A., Al-Zaidy, S., et al. (2020). Assessment of systemic delivery of rAAVrh74.MHCK7.micro-dystrophin in children with Duchenne muscular dystrophy: A nonrandomized controlled trial. JAMA Neurol. *77*, 1122–1131.

46. Lostal, W., Bartoli, M., Bourg, N., Roudaut, C., Bentaïb, A., Miyake, K., Guerchet, N., Fougerousse, F., McNeil, P., and Richard, I. (2010). Efficient recovery of dysferlin deficiency by dual adeno-associated vector-mediated gene transfer. Hum. Mol. Genet. *19*, 1897–1907.

47. Grose, W.E., Clark, K.R., Griffin, D., Malik, V., Shontz, K.M., Montgomery, C.L., Lewis, S., Brown, R.H., Jr., Janssen, P.M.L., Mendell, J.R., et al. (2012). Homologous recombination mediates functional recovery of dysferlin deficiency following AAV5 gene transfer. PLoS One *7*, e39233.

48. Pryadkina, M., Lostal, W., Bourg, N., Charton, K., Roudaut, C., Hirsch, M.L., and Richard, I. (2015). A comparison of AAV strategies distinguishes overlapping vectors for efficient systemic delivery of the 6.2 kb Dysferlin coding sequence. Mol. Ther. Methods Clin. Dev. *2*, 15009.

49. Liu, M., Yue, Y., Harper, S.Q., Grange, R.W., Chamberlain, J.S., and Duan, D. (2005). Adeno- associated virus-mediated microdystrophin expression protects young mdx muscle from contraction-induced injury. Mol. Ther. *11*, 245–256.

50. Wang, Z., Kuhr, C.S., Allen, J.M., Blankinship, M., Gregorevic, P., Chamberlain, J.S., Tapscott, S.J., and Storb, R. (2007). Sustained AAV-mediated dystrophin expression in a canine model of Duchenne muscular dystrophy with a brief course of immunosuppression. Mol. Ther. *15*, 1160–1166.

51. Shin, J.H., Nitahara-Kasahara, Y., Hayashita-Kinoh, H., Ohshima-Hosoyama, S., Kinoshita, K., Chiyo, T., Okada, H., Okada, T., and Takeda, S. (2011). Improvement of cardiac fibrosis in dystrophic mice by rAAV9-mediated microdystrophin transduction. Gene Ther. *18*, 910–919.

52. Bostick, B., Shin, J.H., Yue, Y., and Duan, D. (2011). AAV-microdystrophin therapy improves cardiac performance in aged female mdx mice. Mol. Ther. *19*, 1826–1832.

53. Koo, T., Okada, T., Athanasopoulos, T., Foster, H., Takeda, S., and Dickson, G. (2011). Long- term functional adeno-associated virus-microdystrophin expression in the dystrophic CXMDj dog. J. Gene Med. *13*, 497–506.

54. Shin, J.H., Pan, X., Hakim, C.H., Yang, H.T., Yue, Y., Zhang, K., Terjung, R.L., and Duan, D. (2013). Microdystrophin ameliorates muscular dystrophy in the canine model of duchenne muscular dystrophy. Mol. Ther. *21*, 750–757.

55. Potter, R.A., Griffin, D.A., Heller, K.N., Peterson, E.L., Clark, E.K., Mendell, J.R., and Rodino- Klapac, L.R. (2021). Dose-escalation study of systemically delivered rAAVrh74.MHCK7.micro- dystrophin in the mdx mouse model of Duchenne muscular dystrophy. Hum. Gene Ther. *32*, 375–389.

56. Birch, S.M., Lawlor, M.W., Conlon, T.J., Guo, L.J., Crudele, J.M., Hawkins, E.C., Nghiem, P.P., Ahn, M., Meng, H., Beatka, M.J., et al. (2023). Assessment of systemic AAV- microdystrophin gene therapy in the GRMD model of Duchenne muscular dystrophy. Sci. Transl. Med. *15*, eabo1815.

57. Piepho, A.B., Lowe, J., Cumby, L.R., Dorn, L.E., Lake, D.M., Rastogi, N., Gertzen, M.D., Sturgill, S.L., Odom, G.L., Ziolo, M.T., et al. (2023). Micro-dystrophin gene therapy demonstrates long-term cardiac efficacy in a severe Duchenne muscular dystrophy model. Mol. Ther. Methods Clin. Dev. *28*, 344–354.

58. Llanga, T., Nagy, N., Conatser, L., Dial, C., Sutton, R.B., and Hirsch, M.L. (2017). Structure- based designed nano-dysferlin significantly improves dysferlinopathy in BLA/J mice. Mol. Ther. *25*, 2150–2162.

59. Xu, G.Y., McDonagh, T., Yu, H.A., Nalefski, E.A., Clark, J.D., and Cumming, D.A. (1998). Solution structure and membrane interactions of the C2 domain of cytosolic phospholipase A2. J. Mol. Biol. *280*, 485–500.

60. Roche, J.A., Ru, L.W., O'Neill, A.M., Resneck, W.G., Lovering, R.M., and Bloch, R.J. (2011). Unmasking potential intracellular roles for dysferlin through improved immunolabeling methods. J. Histochem. Cytochem. *59*, 964–975.

61. Gushchina, L.V., Bhattacharya, S., McElhanon, K.E., Choi, J.H., Manring, H., Beck, E.X., Alloush, J., and Weisleder, N. (2017). Treatment with recombinant human MG53 protein increases membrane integrity in a mouse model of limb girdle muscular dystrophy 2B. Mol. Ther. *25*, 2360–2371.

62. Harsini, F.M., Chebrolu, S., Fuson, K.L., White, M.A., Rice, A.M., and Sutton, R.B. (2018). FerA is a membrane-associating four-helix bundle domain in the ferlin family of membrane-fusion proteins. Sci. Rep. *8*, 10949.

63. Dominguez, M.J., McCord, J.J., and Sutton, R.B. (2022). Redefining the architecture of ferlin proteins: Insights into multi-domain protein structure and function. PLoS One *17*, e0270188.

64. Matsuda, C., Miyake, K., Kameyama, K., Keduka, E., Takeshima, H., Imamura, T., Araki, N., Nishino, I., and Hayashi, Y. (2012). The C2A domain in dysferlin is important for association with MG53 (TRIM72). PLoS Curr. *4*, e5035add5038caff5034.

65. Krahn, M., Wein, N., Bartoli, M., Lostal, W., Courrier, S., Bourg-Alibert, N., Nguyen, K., Vial, C., Streichenberger, N., Labelle, V., et al. (2010). A naturally occurring human minidysferlin protein repairs sarcolemmal lesions in a mouse model of dysferlinopathy. Sci. Transl. Med. *2*, 50ra69.

66. Lostal, W., Bartoli, M., Roudaut, C., Bourg, N., Krahn, M., Pryadkina, M., Borel, P., Suel, L., Roche, J.A., Stockholm, D., et al. (2012). Lack of correlation between outcomes of membrane repair assay and correction of dystrophic changes in experimental therapeutic strategy in dysferlinopathy. PLoS One *7*, e38036.

67. Weisleder, N., Takizawa, N., Lin, P., Wang, X., Cao, C., Zhang, Y., Tan, T., Ferrante, C., Zhu, H., Chen, P.-J., et al. (2012). Recombinant MG53 protein modulates therapeutic cell membrane repair in treatment of muscular dystrophy. Sci. Transl. Med. *4*, 139ra85.

68. DiFranco, M., Quinonez, M., Capote, J., and Vergara, J. (2009). DNA transfection of mammalian skeletal muscles using *in vivo* electroporation. J. Vis. Exp. *2009*, 1520.

69. Zhao, Z., Moloughney, J.G., Zhang, S., Komakzaki, S., and Weisleder, N. (2012). Ora1 mediates exacerbated Ca(2+) entry in dystrophic skeletal muscle. PLoS One *7*, e349862.

70. Alloush, J., Roof, S.R., Beck, E.X., Ziolo, M.T., and Weisleder, N. (2013). Expression levels of sarcolemmal membrane repair proteins following prolonged exercise training in mice. Indian J. Biochem. Biophys. *50*, 428–435.